Supplementary Material

We pre-characterized a collection of samples prior to the work described in the manuscript. The goal was to select samples free of cross-hatch structures that are caused by misfit dislocations to relax the lattice mismatch between the substrate and the epilayer. In doing so, we were able to study exclusively the threading dislocations that emerge from substrate towards the epilayer. Figure 1 illustrates the typical misfit dislocation structure manifested by the crosshatch appearance in a LPE-grown MCT layer. Typical lattice mismatch yielding cross-hatch structures was reported as $> 0.02\%$ in LPE-grown layers (Tobin et al. 1995).

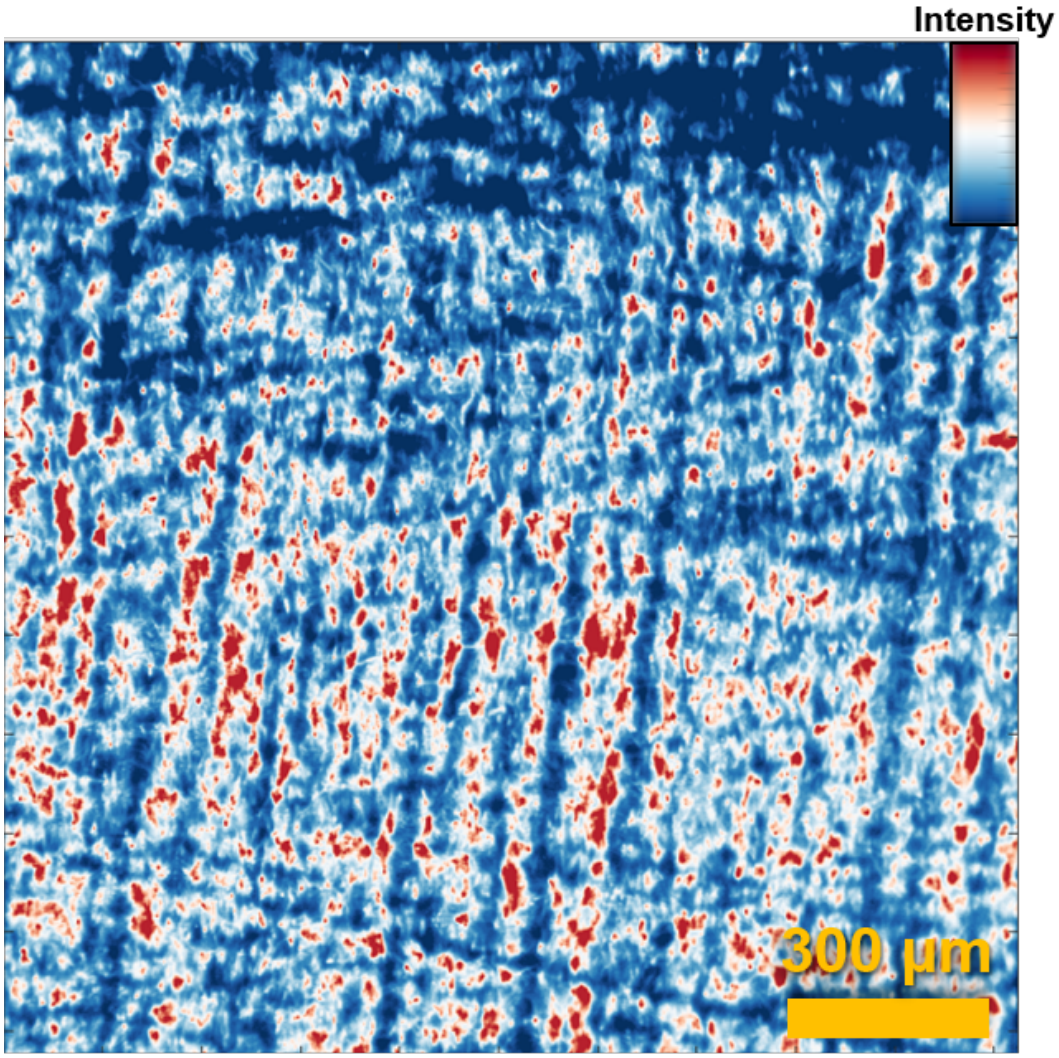

Figure 1: X-ray topography image of an MCT epilayer recorded at the peak position of the rocking curve. The lattice mismatch $> 0.02\%$ shows high density crosshatch pattern of misfit dislocations. Red color shows higher intensity.

We explored three different photon energies to optimize between the X-ray transmission and layer-substrate peak separation.Figure 2 shows the raw images at the weak beam conditions of both

sides of the rocking curves collected at 12 keV and 36 keV photon energies, respectively. At 12 keV, shown in Figure 2 (a) and (b), CZT defects are not visible due to the limited penetration power at higher θ values, unlike what is observed at 15 keV. The attenuation length at 12 keV is calculated as 1.66 μm for $I_x/I_0 = 0.36$, where I_x is the transmitted and I_0 is the incident beam intensity. Therefore the incident beam is absorbed before reaching the CZT substrate and reflecting back. Turning to the images collected at 36 keV, Figure 2 (c) and (d), one can see the threading dislocations in both sides of the rocking curve, thanks to the increased penetration depths. However, the angular separation between the layer and the substrate peaks decreases as the incident photon energy is increased. Therefore, the layer distortions are not resolved at this energy with the same angular steps for each data point of the rocking curve (i.e. 10^{-4}). As a result, we focused our study at 15 keV photon energy. The effective penetration depth is calculated as 41 μm from the images of the section topographs in reflection geometry at 15 keV. Thus at this energy, we could resolve the diffraction contributions of the substrate and the layer to the total rocking curve, separately. All XBDI measurements in the manuscript thus were carried out at 15 keV.

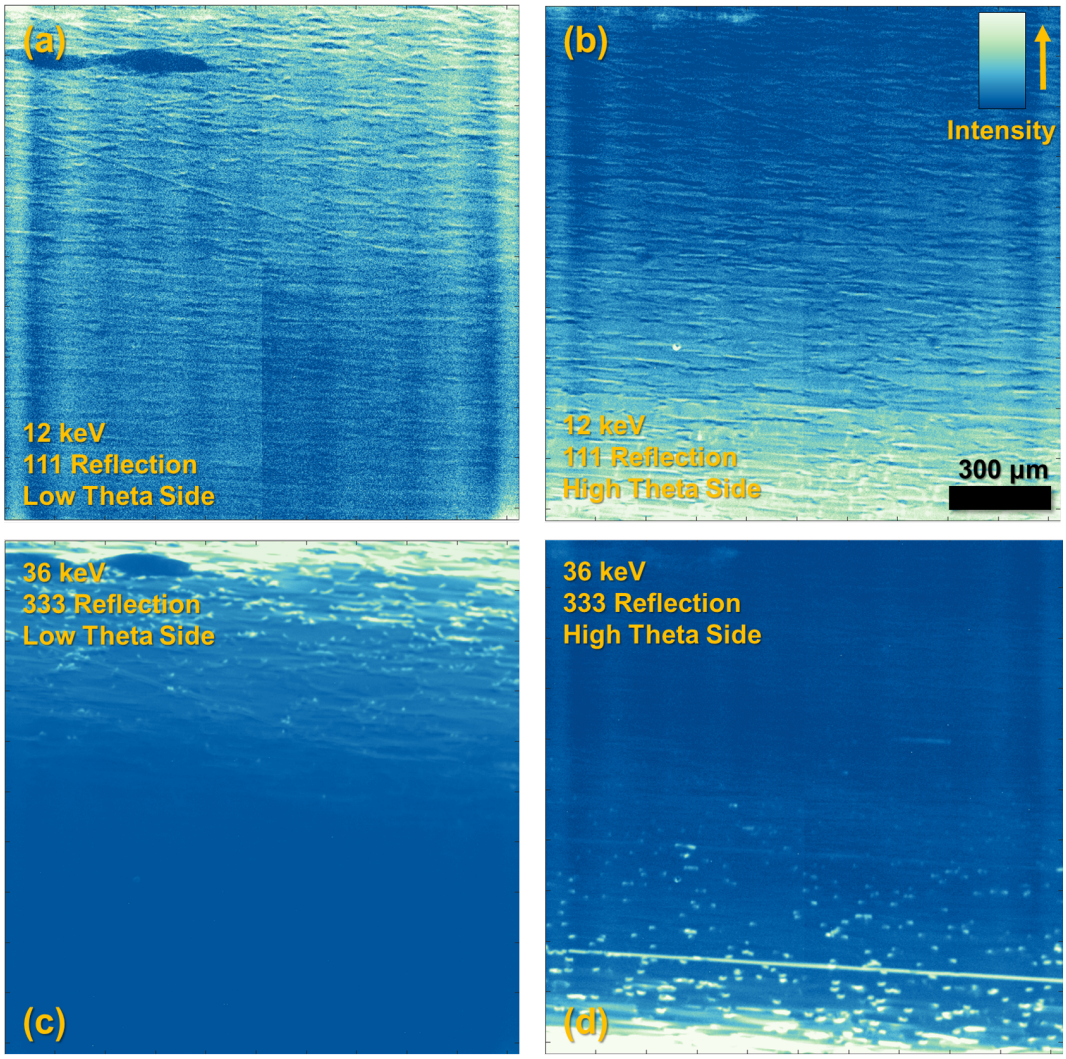

Figure 2: Projection images of the sample at (a) on 111 Bragg reflection at 12 keV at the beginning of the rocking curve (b)on 111 Bragg reflection at 12 keV on the at the end of the rocking curve (c)on 333 reflection at 36 keV at the beginning of the rocking curve (d) on 333 reflection at 36 keV at the end of the rocking curve. Color scale is chosen to give the best contrast and blue color indicates higher intensity. The field of view is 1.5 x 4.5 mm (horizontal x vertical)